2

NASA TECHNICAL TRANSLATION NASA TT F-14481

DESORPTION OF OXYGEN FROM TUNGSTEN BY MEANS OF ELECTRON IMPACT

A. Klopfer

Translation of an article from Vakuum-Technik, Vol. 1, 1970, pp. 1-8.

NATIONAL AERONAUTICS AND SPACE ADMINISTRATION
WASHINGTON, D.C. 20546 JUNE 1972

Special Reprint from Vakuum-Technik, Rudolf A. Lang Press, 627 Idstein PO Box,
Vol. 1/70, pp. 1-8

Desorption of Oxygen From Tungsten by Means of Electron Impact

by A. Klopfer

Summary

The effect of electron impact on oxygen adsorbed on polycrystalline tungsten has been investigated with the aid of mass spectrometers. From these investigations and from thermal desorption and adsorption measurements, the existence of three adsorption states at 430° K has been concluded. Desorption by electron impact from the state in which the oxygen is most strongly bonded to the tungsten could not be detected with certainty. Atomic oxygen ions and neutral particles, which are very probably oxygen atoms, are liberated from the second state. The cross section for the neutral particles is $8 \cdot 10^{-19}$ cm^2; for the ions, $3 \cdot 10^{-21}$ cm^2. Oxygen molecules and atomic oxygen ions were desorbed from the state in which the oxygen is loosely bonded and in which the coverage amounts to only 2% of the total quantity of gas adsorbed. The cross section of electron desorption for O_2 is $1.5 \cdot 10^{-17}$ cm^2; for desorption of O^+, $7 \cdot 10^{-20}$ cm^2.

Introduction

Studies on the dissociation and desorption of neutral and charged particles resulting from the interaction of electrons with solid bodies or with adsorption layers have been being performed since the beginning of this century, wherein the purpose of the study was determined by the particular immediate problem. At the time when the mass spectrometer was being developed, Dempster [1] attempted in 1918 to make use of electron bombardment to analyze solid bodies, with the idea of breaking open the chemical bond by means of electron impact and thereby causing desorption of positive ions. (A review of the material published up to 1967 can be found in [2] and [3]). Some 30 years later, further studies were triggered by contamination phenomena observed on cathodes in electron tubes. Here, the experiments extended to pure anode materials, their oxides, cathode materials, and their vaporization products. The essential finding, as summarized by Plumlee and Smith [4], was that the materials transfer resulting from electron bombardment of solid bodies was indeed negligible, if purely thermal effects are ruled out, but that adsorption layers of electronegative materials give rise to desorption, where ions (e.g. O^+, Cl^+, Cl^-, F^+) are mainly observed as desorption products.

The development of ultra-high-vacuum (UHV) technology stimulated new interest in ion desorption. At very low pressures, the ion flows in the ionization manometers or partial-pressure measurement devices, as caused by the ionization of the gas molecules in the space, may be comparable to or even much smaller than the ion flows caused by electron bombardment of the anodes. The order of magnitude of this effect and its effect on pressure

measurement were studied thoroughly by Redhead [5] in molybdenum and adsorbed oxygen. Lawson [6] extended the investigations, which were carried out in the pressure range from 10^{-8} to several times 10^{-7} torr, to other anode materials, such as platinum, tantalum, and tungsten and found that of the four metals mentioned above, tungsten and platinum are the best-suited anode materials for ionization meters.

Further applications of desorption caused by electron bombardment deal with gas emission [7], the purification of surfaces in vacuum units [8], and the influence on the surface structures observed in LEED experiments [9]. After Menzel and Gomer [10] and Redhead [11] had shown that the cross section of electronic desorption is greatly influenced by the type of bonding of the adsorbed phases, this effect was used as a sensitive method of demonstrating various chemisorption phases.

The desorption by means of electrons of an oxygen layer adsorbed on tungsten was studied by Menzel and Gomer [10] and by Bennette and Swanson [12], with the aid of a field emission electron microscope. This method makes it possible to observe changes in the coating of a tungsten point. Similarly, Zingerman et. al. [13], who used the changes in the work function when oxygen is adsorbed and desorbed on monocrystalline tungsten surfaces as his measurement method, was unable to draw any conclusions about the nature of the desorbed particles. Nor were Madey and Yates [14] able from their measurements, in which the desorbed ion flow served as an indicator, to draw conclusions about the nature of the particles desorbed by means of electron impact from the various adsorption phases.

Consequently, the purpose of this study was to be able to draw some conclusions about the desorbed neutral and ionized particles, by using mass-spectrometric methods, and to study the properties of the various adsorption phases in the oxygen-tungsten system, in combination with adsorption measurements and thermal desorption.

Experiment

The measurements were made in two different UHV devices. The first one, hereinafter called A_N, was specially designed for adsorption measurements and for analyzing the desorbed neutral particles, whereas the second one, A_I, serve to detect the desorbed ions. Fig. 1 shows the schematic design of A_N.

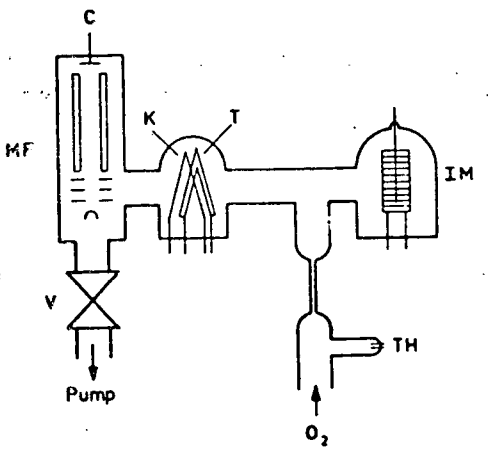

Fig. 1. Measurement device A_N.

T = target (tungsten belt); K = cathode; MF = mass filter; C = ion collector; IM = ionization manometer; TH = thermoelectric vacuometer; V = metal valve to be baked out.

The glass testing tube, whose inner walls were coated with a conducting layer of SnO_2 and which was negative with respect to the cathode, contained a polycrystalline tungsten belt, 25 μ thick, with an area of 0.5 cm^2 exposed to electron bombardment. A 100-μ tungsten wire was used as a cathode; it was mounted parallel to the belt, at a distance of 2 mm. The partial pressures were determined with a quadrupole mass filter. The ionization manometer served to calibrate the mass filter. During the actual tests, it was kept shut off, so as not to unnecessarily bombard surfaces with electrons thus also generating desorption. The test gas flowed in through a capillary of known conductivity and was again pumped out through the valve. In this way, measurements could be made under steady conditions.

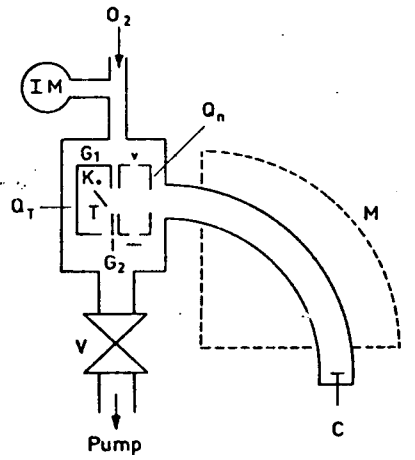

Fig. 2. Measurement device A_I

Q_n = standard ion source; Q_T = target area; T = target; K = cathode; G_1 and G_2 = electrodes; M = magnet; C = ion collector of the mass spectrometer; IM and V same as in Fig. 1.

The second UHV device A_I (Fig. 2) consisted of a 90° sector field mass spectrometer (radius 15 cm) of stainless steel. The partial pressures

could be measured in the standard electron-impact ion source Q_n. Behind it, there was a second source Q_T, within which the target T was bombarded with electrons from the tungsten cathode K. The target, also a polycrystalline tungsten belt, had a $5 \cdot 10^{-2}$ cm^2 area exposed to the electron bombardment. Desorbed ions could be moved directly through the slots within the ion source Q_n into the analyzer. Since the cathode K had a negative voltage of 150 V relative to the target, the ion paths had to be corrected via appropriate voltages at electrodes G_1 and G_2. The voltage at the target was kept constant at +250 V relative to the outer housing of source Qn. Source Qn was calibrated by means of comparison with an ionization manometer. The transmission -- i.e. the ratio of the flow on collector C to the flow leaving the target -- had to be determined for the source Q_T, so as to be able to draw conclusions about the ion flow desorbed by means of electron impacts. For this purpose, the thermal emission of potassium and sodium ions, which appear as impurities in the tungsten before the target is cleaned, was made use of. Thus, ion flows of some 10^{-7} amp from the target could be obtained for an extended period of time. In this way, the transmission was determined to within within 1 °/oo. At the same time, this ion emission served to establish the mass scale for source Q_T.

The ion flow from source Q_T may contain yet another component formed by ionization of the gas molecules in front of the target. However, this component is very insignificant, only becoming noticeable at pressures greater than 10^{-6} torr, as experiments with argon and hydrogen have revealed.

To begin with, the apparatuses were baked and pumped out, according to the usual procedure in UHV technology. Then the target and the tungsten cathodes were cleaned of carbon impurities, in an oxygen atmosphere of

$5 \cdot 10^{-7}$ to $1 \cdot 10^{-6}$ torr, at temperatures around 2000°K. The tests were not begun until the CO partial pressure had dropped to a few percent of the O_2 pressure. The oxygen partial pressure was varied between $5 \cdot 10^{-9}$ and 10^{-6} torr, the electron current density, between 10^{-5} and $2 \cdot 10^{-3}$ amp/cm^2. Since for the maximum electron current used, the temperature of the tungsten belt rose to 430°K, all measurements were made at this temperature.

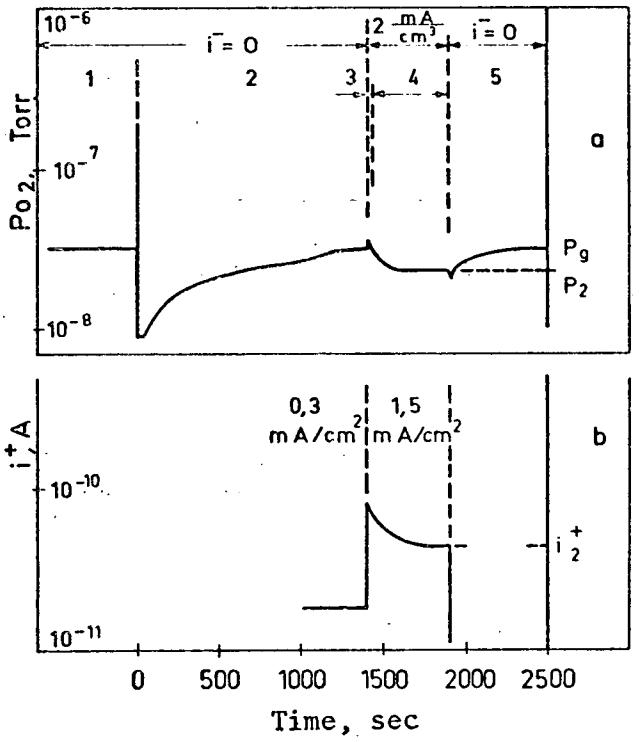

Fig. 3. Time curve of a test run.

a) Variation in oxygen pressure at a constant O_2 inflow rate.
b) Variation in the O^+ ion flow when the electron current is increased; $p_g = 1.5 \cdot 10^{-8}$ torr.

The time curve of a test run in which the gas quantity flowing in per unit of time remained constant is shown in Fig. 3. At first, the O_2 pressure was steadied after the target and cathodes had reached the proper

temperatures. In this time interval 1, the target was not yet being bombarded with electrons. After the target had been decontaminated via short-term superheating to 2300°K, an adsorption curve was plotted (Interval 2). At the end of this interval, the initial pressure was again reached. If now an electron stream was attracted to the target by applying a voltage of 150 V between the target and the cathode, at first, molecular oxygen was desorbed (Interval 3); then the O_2 pressure dropped to a steady value, which, however, was lower than the initial pressure (Interval 4). Only O^+ ions were found as desorbed ions in intervals 3 and 4.

This lowering of the steady pressure can only be explained by saying that the electron impact purified the target of adsorbed particles which were not contributing to the oxygen pressure. The O^+ ion flow is too small by a factor of 100 to have been able to cause this pressure drop. Desorption of neutral atomic oxygen may be viewed as the probable cause. It is extremely difficult to detect this atomic oxygen in the mass spectrometer, since, on the one hand, it is easily adsorbed on the walls of the apparatus, so that the number of ions formed in the ion source is very low, whereas on the other hand, the molecular oxygen also forms O^+ ions in the gas chamber when there are electron impacts. It is totally out of the question to explain the pressure drop in Interval 4 by means of the pumping effect of the ions formed in the gas chamber in front of the target, since the pure ion pumping rate is at most only $4 \cdot 10^{-4}$ ℓ/sec, whereas the example shown in Fig. 3 reveals an additional pumping rate of 0.75 ℓ/sec, caused by electron impact. Nor can the lowering of the steady pressure have been caused by the desorption of tungsten oxides, since Ptushinskii and Chuikow [15] and McCarrol [16], using mass spectrometers, have found that no oxides at all or only very few are

formed during the adsorption of oxygen onto tungsten at room temperature, whereas according to our measurements a total of about one third of the adsorbed oxygen quantity can be desorbed by electron impacts, as will be shown later.

If the electron current is again shut off (Interval 5), this results at first in a slight pressure drop, since now there is no more desorption of the molecularly adsorbed oxygen. Then the pressure rises, until there is once more a complete coating. The gas quantity desorbed during electron bombardment can be determined from this readsorption curve.

Thus, from the measurements we can conclude that when we bombard tungsten upon which oxygen is adsorbed with electrons, O_2 molecules, O^+ ions, and very likely O atoms are desorbed.

The adsorption or desorption rates can be determined from the pressure changes, according to the following expression:

$$\left(\frac{dn}{dt}\right)_{ads} - \left(\frac{dn}{dt}\right)_{des} + K \cdot S_A (p - p_g) + KV \frac{dp}{dt} = 0 \qquad (1)$$

where dn/dt is the number of particles adsorbed or desorbed per second; K is a conversion factor (= $3.2 \cdot 10^{19}$ molecules/torr ℓ); S_A is the pumping rate of the apparatus; V is the volume; and $(p - p_g)$ is the pressure change. The pumping rate of the apparatus can be found from

$$S_A = L \frac{p_v - p_g}{p_g} \qquad (2)$$

where L is the conductivity of the capillary tube and p_v is the oxygen pressure in front of the capillary tube. Integrating Eq. (1) yields the number of adsorbed or desorbed particles.

In order to obtain the parameters for the desorption during electron impact, we use the following expression:

$$\left(\frac{dn}{dt}\right)_m = \frac{i^-}{\varepsilon}\,\Theta_m\,\eta_m = \frac{i^-}{\varepsilon}\cdot N_m\,\sigma_m \tag{3}$$

where the subscript m designates the various adsorption phases; i^- is the impinging electron current; ε is the electron charge; Θ is the relative coating; η is the probability of desorption; N is the number of adsorbed particles per cm^2; and σ is the cross section. Accordingly, we have the following for the desorbed ions:

$$(i^+)_m = i^-\,\Theta_m\,\eta^+_m = i^-\,N_m\,\sigma^+_m \tag{4}$$

The probabilities of desorption are determined when the coating complete ($\Theta = 1$). Whereas σ^+_m can only be calculated from Eq. (4), the cross sections σ_m can be estimated from the pressure drop per unit time or the change in the O^+ ion flow per unit time, without needing to know the extent of coating [11]. If the readsorption can be neglected, integration of Eq. (3) yields the following:

$$N_m = N_A\,e^{-t/\tau_m} \quad \text{with} \quad \tau_m = \frac{1}{\sigma_m \cdot j/\varepsilon} \tag{5}$$

where N_A is the coating present at the time $t = 0$, and j/ε represents the number of electrons impinging per cm^2 and per sec. If we again insert Eq. (5) into Eqs. (3) and (4), we get:

$$\left(\frac{dn}{dt}\right)_m = \frac{i^-}{\varepsilon}\,\sigma_m \cdot N_A\, e^{-t/\tau_m} \tag{6}$$

$$(i^+)_m = i^-\,\sigma_m{}^+ \cdot N_A\, e^{-t/\tau_m} = (i^+_A)_m\, e^{-t/\tau_m} \tag{7}$$

A semilog plot of $(dn/dt)_m$ or $(i^+)_m$ according to time yields a straight line, from which the time constant τ_m can be determined, as well as σ_m -- assuming that the individual adsorption phases can be studied separately. In our case, in which molecular and atomic oxygen were desorbed simultaneously, a corresponding plot of $(p - p_2)$ or $(i^+ - i_2^+)$ -- see Fig. 3, Intervals 3 and 4 -- yielded a curve which dropped rapidly at the beginning and then became a straight line. Extrapolation of these straight lines up to $t = 0$, followed by a semilog plot of the difference between the measured curve and the extrapolated straight lines yielded a new straight line which we assign to the desorption of O_2, with a time constant of 5 to 10 sec, whereas about 100 sec was obtained for the O desorption.

Results

The adsorption phase from which O_2 molecules are desorbed upon electron impact and which shall hereinafter be designated as Phase I, exhibits to some extent a behavior similar to that described by Singleton [19]

for the phase which he designated as β_1. Occupation of this phase -- which we derive from the desorption experiments -- is a function of the product of the oxygen pressure and the gas-treatment time and depends only slightly on the oxygen pressure if this product is kept constant. The number of O_2 molecules desorbed by electron impacts was estimated by means of the area under the O_2 desorption curve (Fig. 3, Interval 3), taking into account the contribution made by simultaneous O desorption, and by means of the readsorption after the electron flow was shut off (initial pressure drop in Interval 5).

At an oxygen pressure p_g of $3 \cdot 10^{-8}$ torr, electron impact desorbed $3 \cdot 10^{12}$ molecules per cm^2, after a gas-treatment time of 1200 sec; whereas after $2 \cdot 10^4$ sec, we estimated $1.4 \cdot 10^{13}$ molecules per cm^2. At a pressure of $1.2 \cdot 10^{-6}$ torr and a gas-treatment time of 400 sec, we got $1.2 \cdot 10^{13}$ molecules per cm^2. Thermal desorption at desorption temperatures greater than 1200°K yields similar values, within a factor of 2. If the temperature is raised to 600°K after adsorption with $p_g = 1.2 \cdot 10^{-6}$ torr at 430°K, there follows further adsorption of $1 \cdot 10^{14}$ molecules per cm^2, with an initial probability of adhesion of 0.02. Almost the same number of oxygen molecules could be redesorbed after turning the electron current on, with a desorption probability of $8 \cdot 10^{-4}$ molecules per electron. The cross section which was determined from the pressure drop and from the drop in ion flow between 1 and $2 \cdot 10^{-17}$ cm^2 did not exhibit any dependence of this kind. The number of O_2 molecules desorbed per cm^2 by means of electron impact was equal to the number N of adsorbed molecules per cm^2 resulting from Eq. (3), with the measured values for dn/dt, i^-, and σ. Since, moreover, the O^+ ion flow with a full coating is linear with the

electron current, and the cross section of desorption for O_2 molecules is greater than that for O desorption by more than a factor of 10, it is probable that in this adsorption phase the oxygen is adsorbed on the tungsten surface in molecular form.

In addition to this adsorption phase, there is still another phase which can be emptied by means of electron impact. This phase will hereinafter be designated as Phase II. The drop in the steady pressure p_g to the lower value p_2 under electron bombardment (Fig. 3) is explained by the desorption of atomic oxygen. Since in the steady condition the adsorption rate must equal the desorption rate, using Eq. (1) yields the desorption rate $(dn/dt)_{II}$ according to the following equation:

$$\left(\frac{dn}{dt}\right)_{II} = 2\left(\frac{dn}{dt}\right)_{O_2} = 2\,KS_A\,(p_g - p_2) \qquad (8)$$

Fig. 4 shows $(dn/dt)_{II}$ and the number of O+ ions desorbed per second as a function of the O_2 pressure p_2. The number of O ions was converted for an electron current of 1 ma at high pressures and for an area of $5 \cdot 10^{-1}$ cm^2 in the low-pressure range, in order to make a comparison with the O desorption. At high pressures, they reach a constant value and become a linear function of the electron current. At low pressures, on the other hand, the desorption rates become independent of the electron current and become a linear function of the pressure. This means that in the high-pressure range -- that is, where $\Theta = 1$ -- the desorption rate is the decisive step, whereas in the low pressure range, it is the adsorption rate. The desorption probabilities were determined from the measurements made at high pressures;

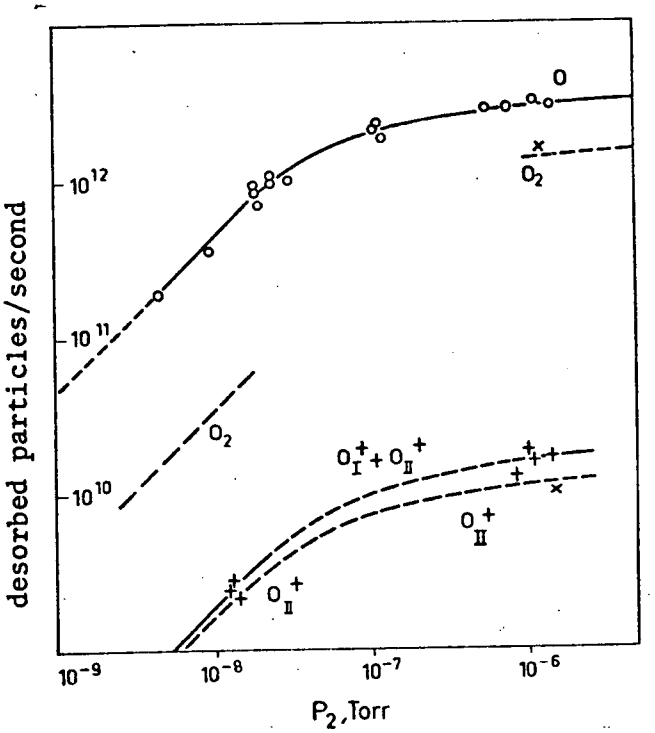

Fig. 4. Number of desorbed particles per second during electron bombardment with 1 ma, 150 V, as a function of the oxygen pressure (under steady conditions).

O = oxygen atoms; O_2 = oxygen molecules (dashed line calculated)
$O_I^+ + O_{II}^+$ = total ion flow; O_{II}^+ = ion flow from Phase II (dashed line calculated).

according to Eqs. (3) and (4), they were calculated to be $\eta_{II} = 5 \cdot 10^{-4}$ oxygen atoms per electron, and $\eta_{II}^+ = 2 \cdot 10^{-6}$ O^+ ions per electron. A mean value of $8 \cdot 10^{-19}$ cm^2 was obtained for the cross section σ_{II}. Now, according to Eq. (3), with a full coating ($\theta = 1$), the number of adsorbed O atoms for Phase II can be calculated:

$$N_{II} = \frac{\eta_{II}}{\sigma_{II}} = 6{,}3 \cdot 10^{14} \quad \text{atoms/cm}^2$$

as well as, in turn, the cross section for ion desorption:

$$\sigma_{II}^{+} = \frac{\eta_{II}^{+}}{N_{II}} = 3{,}2 \cdot 10^{-21}\ \mathrm{cm}^2.$$

The number of atoms adsorbed in Phase II was also determined according to readsorption measurements (Fig. 3, Interval 5), after Phase II had been drained to a relative coverage of about 20% at low pressures, with a suitable choice of electron current. Since the readsorbed oxygen quantity is proportional to $1 - \Theta$, we get the maximum coverage, converted for $\Theta = 1$. The measurement values were between $2.65 \cdot 10^{14}$ and $3.1 \cdot 10^{14}$ molecules per cm^2 -- values which agree quite well with the value of $6.3 \cdot 10^{14}$ atoms per cm^2 calculated from η and σ.

The adhesion probability, as a function of the absolute or relative coating [11], can be determined from the measurements in the steady state, with different pressures or different electron currents, since the adsorption rate $(dn/dt)_{O_2}$ can be expressed by

$$\left(\frac{dn}{dt}\right)_{O_2} = F\,(pvs)_{O_2} \qquad (9)$$

where F is the area of the tungsten belt impinged upon by electrons; p is the oxygen pressure; ν is the specific impingment rate ($= 3.5 \cdot 10^{20}$ molecules/cm^2-sec-torr); and s is the adhesion probability. The coating value can be calculated from Eqs. (3) and (8):

$$\Theta_{II} = 2\left(\frac{dn}{dt}\right)_{O_2} \cdot \frac{F}{i \cdot \eta_{II}} \quad \text{and}$$

$$N_{II} = 2\left(\frac{dn}{dt}\right)_{O_2} \cdot \frac{F}{i \cdot \sigma_{II}} \tag{10}$$

Similarly, the adhesion probability can be determined from the O^+ ion flow if Eqs. (9) and (10) are inserted into Eq. (4).

$$s = \frac{i_{II}^+}{2\,Fpv\varepsilon} \cdot \frac{\eta_{II}}{\eta_{II}^+} = \frac{i_{II}^+}{2\,Fpv\varepsilon} \cdot \frac{\sigma_{II}}{\sigma_{II}^+}$$

The proportion of the O^+ ion flows stemming from Phase II was determined by means of the above-mentioned semilog graph of the drop in the ion flow with time after the gas was pumped out. The coating values were calculated from Eq. (4). Fig. 5 graphs the adhesion probabilities obtained in this way, as well as those obtained from readsorption measurements, as a function of the relative coating in Phase II and as a function of the total absolute coating (Curve b). The total absolute coating and the corresponding adhesion probabilities (Curve a) result from the adsorption curve (Fig. 3, Interval 2) which was recorded after thermal desorption at 2300°K. The differences in coating between Curves a and b indicate an additional adsorption phase (hereinafter called Phase III), which is not influenced at all or is only slightly influenced by electron bombardment, thus agreeing with the findings of Menzel and Gomer [10] and those of Madey and Yates [14]. These latter authors observed a positive ion flow during

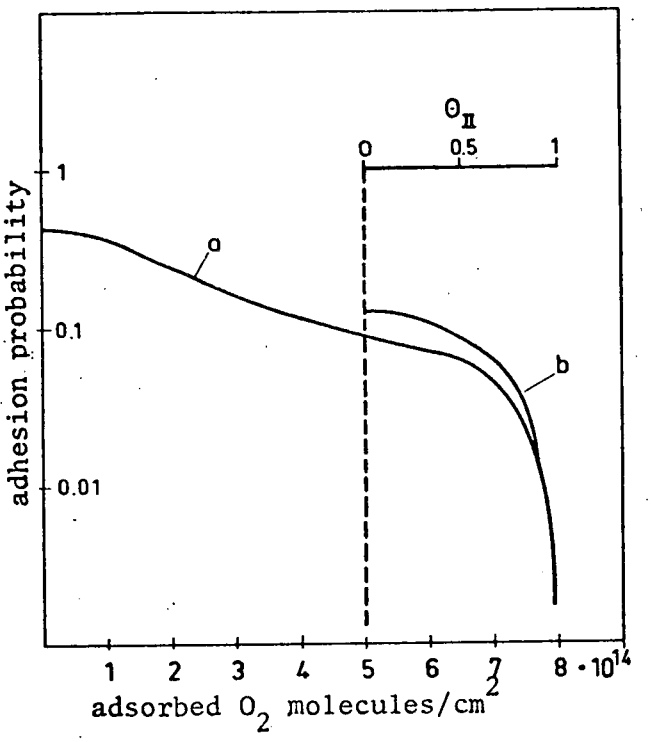

Fig. 5. Adhesion probability for oxygen on tungsten, as a function of coverage.

Curve (a): obtained from the adsorption measurement (Fig. 3, Interval 2)
Curve (b): --+-- readsorption measurement after bombardment with electrons.
--(•)-- computed from the desorption values under bombardment with electrons (Fig. 3, Interval 4)

electron bombardment only after the adsorption of $2.5 \cdot 10^{14}$ molecules/cm^2. Similarly, in our studies, when we temporarily turned on the electron current while recording the adsorption curves, it turned out that a noticeable pressure drop only occurred after the adsorption of $4 \cdot 10^{14}$ molecules/cm^2 -- a drop which was interpreted as the desorption of neutral atomic oxygen.

Consequently, during adsorption, Phase III has first occupation priority; only when this phase is almost fully occupied does Phase II

begin to fill up. Ptushinskii and Chuikow [15] report very similar behavior; at concentrations which were not too high, after adsorption at room temperature, they observed only thermal desorption of atomic oxygen with a time-of-flight mass spectrometer. At higher concentrations, the number of desorbed O atoms no longer varies with the coverage, and the tungsten oxides WO_2 and WO_3 appear as desorption products, where the desorption rate rises proportionally with the coating value. From these and other studies they conclude that almost two thirds of the adsorbed oxygen exists in the form of atoms on the surface, bonded with an energy of 6 eV, whereas no definite statements can be made about the adsorption state of the remaining quantity of oxygen. McCarroll [16], on the other hand, observed desorbed oxides making up only about 1% of the desorbed O atoms. The oxides, for which a desorption energy of about 4 eV was found, are formed, according to [15], only after the tungsten has been superheated. Studies of (110)-monocrystal surfaces reveal that here oxides are formed [17] already at room temperature, or else, according to Germer and May [18], there is regrouping of the surface atoms.

We can surely accept as certain the fact that the oxygen in Phase III is present in atomic form, where one oxygen atom is adsorbed per tungsten atom on the surface, if we assume that the orientation at the surface is the same as that inside the tungsten belt. Structural studies with X rays have shown that many low-labeled planes exist having an orientation parallel to the surface.

No conclusions can be drawn from these studies about the adsorption state in Phase II. Desorption tests by means of short-term superheating of

the tungsten belt revealed that at most only 10% of the adsorbed oxygen appears in the gas phase; this can be explained partly by oxygen desorbed from Phase I, partly by recombination of atomically desorbed oxygen [15]. It was not possible to detect atomic oxygen or tungsten oxides with the apparatus used here. Since, however, after superheating to a temperature of 1700°K -- at which still only little atomic oxygen was being desorbed, although the oxides were being desorbed -- the remaining coating, which, as in Singleton [19], was determined from readsorption measurements at low temperatures, was of the same order of magnitude as the remaining coating found by Ptushinskii and Chuikov by means of desorption at very high temperatures, it is quite probable that Phase II is identical with the phase from which the oxides are being desorbed.

Madey and Yates [14], who designate Singleton et. al.'s Phase II as β_1, tend -- on the basis of the model of electron desorption developed by Menzel and Gomer [10], as well as by Redhead [11] -- toward the view that here the oxygen is being adsorbed in molecular form.

This model states that the Frank-Condon excitation of the adsorbed particles by inelastic interactions with the electrons leads to an ionized state with a cross section which is "normal" -- i.e. has the same order of magnitude as in the gas phase -- but that on the other hand the ionized particle, due to tunnel processes, is again neutralized by the surface barrier before it can leave the surface. Desorption becomes more probable, the broader the barrier, that is, the greater the distance between the adsorbed particle and the surface. These concepts could explain the findings observed in the tungsten-oxygen system concerning desorption under electron impact. In Phase III, in which the oxygen atoms are most strongly

Table I

Phase	adsorbed O_2 mol./cm^2	s	η particles/ electron	σ cm^2	desorbed particles	electron energy, eV	T °K	Ref.
I	$1,5 \cdot 10^{13}$	~ 0,02	$1,5 \cdot 10^{-4}$ $1 \cdot 10^{-6}$	$\sim 1,5 \cdot 10^{-17}$ $\sim 7 \cdot 10^{-20}$	O_2 O^+			author's results
II	$3 \cdot 10^{14}$	0,13	$5 \cdot 10^{-4}$ $2 \cdot 10^{-6}$	$8 \cdot 10^{-19}$ $3 \cdot 10^{-21}$	O O^+	150	430	
III		0,42						
II III				$4,5 \cdot 10^{-19}$ $\leq 2 \cdot 10^{-21}$		100	20	[10]
				$3 \cdot 10^{-19}$		100	77	[12]
β_1 β_2	$1,4 \cdot 10^{13}$ $4,9 \cdot 10^{14}$	$> 0,1$ 0,5	$1,5 \cdot 10^{-6}$	$7 \cdot 10^{-19}$ $3,4 \cdot 10^{-20}$ $\leq 2 \cdot 10^{-23}$	neutral p. ions ions	100	300	[14]
(100) (111) (110)				$\sim 6,5 \cdot 10^{-20}$ $\sim 6,5 \cdot 10^{-20}$ $\sim 6,5 \cdot 10^{-21}$		150		[13]

Table I

s = initial probabality of adhesion
η = probability of desorption
σ = cross section of desorption

[Translator's note: In the table, commas represent decimal points.]

bonded and are therefore in very close contact with the metal base, the barrier is so thin that the desorption probability drops to zero or becomes very small. For Phase II, during which only about 1% of the total desorbed particles leave the surface as ions, there already result noticeable cross sections, either because the oxygen is adsorbed in molecular form or because the bonding of oxygen atoms is looser, due to the higher concentration [16].

Possibly Phase I, where the greatest cross sections were obtained, can be characterized as a "forerunner" of chemisorption [21] at concentrations which are not too high and/or as a "gap-filler" [20].

Table I presents a summary and comparison of various findings on electron-impact desorption in the oxygen-tungsten system. If we ignore the values calculated from the data of Zingerman et. al. [13], the total cross sections for Phase II exhibit very good agreement. The larger deviations in the cross sections for ion desorption may in some cases be attributed to different classifications of the adsorption phases. The existence of an additional adsorption phase (Phase III), leading to little or no desorption under electron impact, is found in agreement with Menzel et. al. [10] and Madey et. al. [14].

I thank Mr. H. Fust and Mr. S. Hanloh for carrying out the measurements.

References

[1] A. J. Dempster, Phys. Rev. *11* (1918), 316.

[2] D. Lichtman and R. B. McQuestan, Progress in Nuclear Energy, Series IX, Vol. 4, Pergamon Press 1965.

[3] P. A. Redhead, J. P. Hobson and E. V. Kornelsen, The Physical Basis of Ultrahigh Vacuum, Chapman & Hall Ltd., London, 1968, pp. 168-181.

[4] R. H. Plumlee and L. P. Smith, J. Appl. Phys. *21* (1950), 811.

[5] P. Q. Redhead, Vacuum *13* (1963), 253.

[6] R. W. Lawson, Brit. J. Appl. Phys. *18* (1967), 1763.

[7] G. E. Fischer and R. A. Mack, J. Vac. Sci. Techn. *2* (1965), 123.

[8] G. M. McCracken, R. S. Barton and W. Dillon, Supp. Nuovo Cim. *5* (1967), 146.

[9] J. Anderson and P. J. Estrup, Surface Science *8-9* (1968), 463.

[10] D. Menzel and R. Gomer, J. Chem. Phys. *41* (1964), 3311.

[11] P. A. Redhead, Can. J. Phys. *42* (1964), 886.

[12] C. J. Bennette and L. W. Swanson, J. Appl. Phys. (1965), 2749.

[13] Ya. P. Zingerman and V. A. Ishchuk, Sov. Phys.-Sol. State *8* (1967), 2394; *9* (1967), 623; *9* (1967), 2638.

[14] T. E. Madey and J. T. Yates, Surface Sci. *11* (1968), 327.

[15] Yu. G. Ptushinskii and B. A. Chuikov, Surface Science *6* (1967), 42.

[16] Bruce McCarroll, J. Chem. Phys. *46* (1967), 863.

[17] N. P. Vas'ko, Yu. G. Ptushinskii, B. A. Chuikov, Surface Science *14* (1969), 448.

[18] L. H. Germer, J. W. May, Surface Science *4* (1966), 452.

[19] J. H. Singleton, J. Chem. Phys. *47* (1967), 73.

[20] P. A. Readhead, Trans. Faraday Soc. *57* (1961), 641.

[21] D. O. Hayward, B. M. W. Trapnell, Chemisorption, Butterworths, London, 1964.

Translated for NASA Ames Research Center under Purchase Order No. RO/A-52643A
by LEO KANNER ASSOCIATES, PO Box 5187, Redwood City, CA, 94064, Tel. (415)365-3046
August 1970